

Resonance transmission through a single atom

José-Luis Mozos^(1,a), C.C. Wan⁽¹⁾, Gianni Taraschi⁽¹⁾, Jian Wang⁽²⁾, and Hong Guo⁽¹⁾

(1) *Centre for the Physics of Materials and Department of Physics, McGill University,*

Montreal, Quebec, Canada H3A 2T8.

(2) *Department of Physics, The University of Hong Kong, Pokfulam Road, Hong Kong.*

Abstract

When a single atom is sandwiched in between two electrodes, an *atomic* tunneling device may be realized depending on the distance between the atom and the electrodes. We have performed first-principles pseudopotential calculation in conjunction with a three-dimensional evaluation of the quantum scattering matrix for such a device. We predict the quantum conductance and resonance transmission properties of the Si and Al atomic tunneling devices.

73.40.Cg, 61.16.Ch, 73.20.At, 73.40.-c

Exploiting the band gap differences of various compound semiconductors such as GaAs and AlGaAs, resonance tunneling devices have been fabricated and extensively investigated since the original work of Esaki [1]. A tunneling device may give rise to negative differential resistance due to a quantum resonance, leading to useful electronic applications. In this work, we propose and theoretically analyze a different kind tunneling device, namely *atomic* scale tunneling systems. Rather than resonant transmitting through the quasi-bound states inside a double barrier tunneling structure, in the atomic system a resonance is through atomic orbitals. Since atomic orbitals have energy spacings in the range of eV, the quantum resonance will not be smeared out by a room temperature. Hence in principle room temperature quantum resonance tunneling devices can be achieved. Our work is encouraged by the measurements using scanning tunneling microscope (STM) on quantum conduction through atomic scale tip-substrate systems [2], where quantized conductance is indeed observed at room temperature.

We propose an atomic tunneling structure as shown schematically in the inset of Fig. (3). The essential part of the structure consists of two metallic electrodes sandwiching a single atom in between. The whole system could in principle be fabricated on top of an insulating substrate by micro-fabricating two electrodes and placing an atom in between using the atomic manipulation ability of STM. Fixing the distance between the atom and the electrode, d , vacuum barriers can be established on the two sides of the atom, thus a double-barrier atomic tunneling (DBAT) device is established [3]. The idea of using vacuum barriers to establish a tunnel junction is widely used in STM [4], but an DBAT structure as an atomic quantum functional device is very interesting indeed. The main task of our work, to be presented below, is to predict quantum conductance of the DBAT device for various values of d , to investigate the formation of a atomic quantum point contact as d is reduced thus diminishing the vacuum barriers, and to examine issues which arise when transport is mediated by atomic levels. Although we have concentrated on DBAT devices operated on a single atom, the idea can be extended to clusters, molecules, or other groups of atoms.

To capture the atomic degrees of freedom, we have combined the *ab initio* pseudopotential

total energy method with a three-dimensional (3D) quantum scattering evaluation of the transmission probabilities [5]. First, we solve the *ground state* properties of the atom *and* the two leads by minimizing the Kohn-Sham total energy functional using a plane-wave basis set [6]. The equilibrium analysis produces the self-consistent effective potential $V_{eff}(\mathbf{r}) \equiv \delta U / \delta \rho(\mathbf{r})$ which is seen by all the electrons. Here $U[\rho]$ is the total self-consistent potential energy while ρ the electron density. Second, we evaluate the scattering matrix of an electron traversing the system defined by V_{eff} , by solving a 3D scattering problem using a transfer matrix technique [7]. From the scattering matrix we obtain conductance from the Landauer formula [8].

We have focused on DBAT devices made of Si and Al atoms and used pseudopotentials of Refs. [9,10] for the core, and the parameterization of Ref. [11] for the exchange-correlation term. The leads are modeled by the jellium model. For Si, a jellium lead has a cross section area of $7.25 \times 7.25(a.u.)^2$, length $L = 30.78a.u.$, and its charge is specified [12] by $r_s \approx 2.0a.u.$, mimicking metallic leads. The supercell volume used in our plane-wave based *ab initio* calculations is $21.77 \times 21.77 \times 2(L + d) (a.u.)^3$. For the Al DBAT device, the lead has a cross section area of $8.79 \times 8.79(a.u.)^2$, length $L = 23.57a.u.$, charge density specified by $r_s \approx 2.07a.u.$. The supercell size for the Al DBAT device is $16.67 \times 16.67 \times 2(L + d) (a.u.)^3$. The DBAT setup with square shaped leads has a symmetry of space group D4h. We have used an upper energy cutoff of 8 Rydbergs [13].

For a single adatom on top of a high density jellium substrate, previous calculations showed [14] that the equilibrium jellium-atom bond length is 2.3a.u. for Si, and 2.6a.u. for Al [12]. Hence for values of d greater than these values, a vacuum barrier may be established. Fig. (1) shows the V_{eff} for a Si DBAT device with $d = 6.9 a.u.$. V_{eff} in the 3D leads is essentially a potential well with a depth $\sim -0.50a.u.$ below the Fermi level of the system. From V_{eff} it is clear that the atom is quite isolated from the leads by the vacuum barriers. Reducing d to 3.45 and 4.6a.u., a lower vacuum barrier is obtained as expected. Similar behavior is found for Al DBAT devices. In Fig. (1), the sharp peak at the atomic position reflects the repulsive atomic core, and surrounding the core there is the usual attractive part

of the atomic potential.

Figs. (2,3) show the conductance G for a number of Si and Al DBAT devices which differ by the jellium-atom junction distance d . When d takes the value of equilibrium jellium-atom bond length, $G(E)$ shows the expected “quantized” conductance [15] for quasi-1D quantum wires. However a striking result is the apparent resonance transmission when the atom is isolated inside the DBAT device by the barriers. For both Si and Al systems, the larger the d , the sharper the resonances. This is because a larger d corresponds to a more isolated atom. The resonance peaks must come from the atomic orbitals since the DBAT device is operating on the electronic structure of the single atom. For a Si atom, the valence configuration is $3s^2 3p^2$. Thus the equilibrium “Fermi” energy for an isolated atom should be located at the $3p$ atomic level. For all the Si DBAT devices, our calculated $E_f \approx -0.10$ a.u., which is very close to the higher energy peak position of Fig. (2). This allows us to identify the resonance peak near $-0.09 \sim -0.10$ a.u. as due to the $3p$ atomic orbital. For the largest d we studied, *e.g.* $d = 6.9$ a.u., the sharp $3p$ resonance is split into two nearby peaks as shown in Fig. (2). It is not difficult to understand this splitting when we realize that the $3p$ state is triply degenerate, and its rotational symmetry is broken by the presence of the squared shaped leads which is along the z -direction. Hence for the single $3p_z$ state, the resonance is marked by $G(E_{3p_z}) \approx 1$ in units of $2e^2/h$. On the other hand, the D_{4h} space group respects the rotational symmetry in the $x - y$ direction, thus the degenerate $3p_{x,y}$ states give $G(E_{3p_{xy}}) \approx 2$. The reason that these peaks are slightly higher than 1 and 2 is due to the partial overlap of the states, as is clearly seen in Fig. (2). When the lead-atom distance d is smaller, such as $d = 3.45$ a.u. and 4.6 a.u., the atom is not as isolated. For these cases, the resonance width is larger which smears out the $3p$ splits. As a result, the three states of $3p$ atomic orbital gives a $G(E_{3p}) = 3 \times (2e^2/h)$ resonance.

After understanding the $3p$ resonance peak, it is clear that the lower energy peak of Fig. (2) must result from the $3s$ atomic state. Indeed, since $3s$ is a singlet, we have $G(E_{3s}) = 1 \times (2e^2/h)$. For $d = 6.9$ a.u., the $3s$ peak is extremely sharp, we reproduce it in the inset of Fig. (2). A crucial numerical test of these results is the distance between

the peak positions. For a single Si atom, LDA calculation [16] gives energy level spacing between the $3s$ and $3p$ states to be 0.245a.u.. Our conductance calculation, as shown in Fig. (2), gives the $3s - 3p$ resonance distance in almost perfect agreement with the LDA spectra, with only small differences due to the level splitting and the presence of the leads. Hence it is unambiguous that the transport in a single atom DBAT device is mediated by the atomic levels. For Al DBAT devices, as shown in Fig. (3), all the results give a physical picture which is consistent with that of the Si system, including the quantitative value of the $3s$ - $3p$ resonance peak distance. For different values of d , there is a small but noticeable shift of the relative peak positions (see Figs. (2,3)). This is due to the coupling of the atom to the leads, and can be understood from previous model calculations [17]. Finally, Figs. (2,3) shows the formation of a transmissive quantum point contact: by reducing d to the equilibrium bond length between the atom and the leads, the resonance transmission crosses over to the usual quantized conductance with a quasi-1D nature.

Certain features of the *ab initio* results can be understood analytically. First, it can be generally shown [18] that for 3D resonance tunneling through a symmetric double barrier potential, the peak value of the conductance $G(E)$ for an isolated singlet state is universally $2e^2/h$. The $3s$ peak shows this result. Second, using the discussion of Ref. [18] and Fermi's golden rule, it's not difficult to obtain the resonance width as

$$\Gamma = 2\pi \sum_j |M_j|^2 \delta(E_r - E_j) = \hbar \sum_j w_j,$$

where w_j is the tunneling rate from the atomic resonance level E_r to the lead level E_j , and M_j is the corresponding tunneling matrix element from E_r to E_j . Since the tunneling rate decreases exponentially with the barrier size, we expect the resonance widths to do the same, which is clearly seen in our numerical results. Third, we can understand why the $3p_z$ resonance peak width is wider than that of the $3p_{xy}$ peak. Using a first-order approximation for the tunneling matrix [19]

$$M_j = \int \chi_j^* V_{lead} \phi_r d^3r,$$

where χ_j is the lead state, ϕ_r is the atomic state, and V_{lead} is the potential due to the lead. By approximating the lead wavefunctions with finite square well wavefunctions, and V_{lead} as a potential well, we find $\Gamma_{p_z}/\Gamma_{p_{xy}} = 6.2$ for $d = 6.9a.u.$ This agrees well with the value of 6.0 from our *ab initio* calculation. We thus conclude, that the $3p_z$ resonance peak width is wider than that of the $3p_{x,y}$ peak, because the overlap of the $3p_z$ state with the lead wavefunctions is much larger than the corresponding overlap for the $3p_{xy}$ states.

In summary, we have proposed and theoretically investigated atomic scale double barrier tunneling devices. The quantum resonance transmission in this system is through atomic orbitals, thus conductances obtained characterizes the conduction through a single atom and reveals the valence atomic spectra. Finally we comment that the curves of $G = G(E)$ are useful for giving a first estimate of the electrical current as a function of a voltage across the DBAT device: one obtains the current in the usual fashion by integrating $G(E)$ over energy convoluted with a Fermi function. The importance of the atomic DBAT device lies in the fact that the quantum resonances are observable at room temperature due to the large energy scales (eV) associated with the atomic system. Indeed, with the nonlinear conductance behavior of the DBAT device, many applications can be envisioned.

ACKNOWLEDGMENTS

We gratefully acknowledge financial support by NSERC of Canada and FCAR of Quebec. J. Wang is supported by a RGC grant of the Hong Kong Government under grant number HKU 261/95P, and a research grant from the Croucher Foundation. We thank the Computing Center of University of Hong Kong for a substantial CPU allocation on their IBM SP2 parallel computer for the numerical analysis presented here.

REFERENCES

- ^{a)}Present address: Fritz-Haber-Institut der Max-Planck-Gesellschaft, Faradayweg 4-6, D-14195 Berlin-Dahlem, Germany
- [1] L. Esaki, Phys. Rev. **109**, 603 (1958).
 - [2] J.I. Pascual, *et. l.* Science, **267**, 1793 (1995); E.S. Snow, D. Park, and P.M. Campbell, Appl. Phys. Lett. **69**, 269 (1996); Ali Yazdani, D.M. Eigler, N.D. Lang, Science, Vol. **272**, 1921 (1996).
 - [3] Recently Lang has discussed another possible way to establish a tunnel junction by inserting spacer atoms between the electrodes to isolate the metal atom which mediates the transport. See, N.D. Lang, Phys. Rev. B. **55**, 9364 (1997).
 - [4] I. W. Lyo and Ph. Avouris, Science **245**, 1369 (1989); Ph. Avouris, I.W. Lyo, F. Bozso and E. Kaxiras, J. Vac. Sci. Technol. A **8**, 3405 (1990).
 - [5] C.C. Wan, José-Luis Mozos, Gianni Taraschi, Jian Wang and Hong Guo, Appl. Phys. Lett. **71**, 419 (1997).
 - [6] M.C. Payne, M.P. Teter, D.C. Allan, T.A. Arias and J.D. Joannopoulos, Rev. Mod. Phys. **64**, 1045 (1992).
 - [7] W.D. Sheng, J.B. Xia, Phys. Letts. A **220**, 268(1996).
 - [8] R. Landauer, IBM J. Res. Dev. **1**, 233 (1957).
 - [9] J. Ihm and M.L. Cohen, Solid State Commun., **29**, 711(1979).
 - [10] L. Goodwin, R.J. Needs and V. Heine, J. Phys.: Condens. Matter **2**, 351 (1990).
 - [11] S. Goedecker, M. Teter and J. Hutter, Phys. Rev. B. **54**, 1703 (1996).
 - [12] N.D. Lang, Phys. Rev. B. **52**, 5335 (1995);
 - [13] We present results in atomic units through out this work.

- [14] N.D. Lang and A.R. Williams, Phys. Rev. B **18**, 616 (1978).
- [15] The quantization plateau is not perfect, because the single atom junction is too short to establish perfect quasi-1D transport channels. For a discussion concerning the establishment of quasi-1D behavior, see Ref. [5].
- [16] We obtained the DFT results from the NIST Basic Reference Data for Electronic Structure Calculations Database (<http://math.nist.gov/DFTdata/>). We have also independently verified the quoted value.
- [17] Yongjiang Wang, Jian Wang and Hong Guo, Appl. Phys. Lett. **65**, 1793 (1994).
- [18] V. Kalmeyer and R.B. Laughlin, Phys. Rev. B **35**, 9805 (1987).
- [19] C.J. Chen, *Introduction to Scanning Tunneling Microscopy* (Oxford, New York, 1993), p. 68.

FIGURES

FIG. 1. Effective potential V_{eff} for a single atom Si DBAT device. The atom-lead distance is fixed at $d = 6.9\text{a.u.}$. The vacuum barriers are clearly seen.

FIG. 2. Conductance $G(E)$ as a function of incoming electron energy E for Si DBAT devices. Dashed line: for $d = 2.3\text{a.u.}$, which is the equilibrium atom-leads distance; dotted line: for $d = 3.45\text{a.u.}$; long dashed line: for $d = 4.6\text{a.u.}$; solid line: for $d = 6.9\text{a.u.}$. Inset: resolving the $3s$ resonance peak for the $d = 6.9\text{a.u.}$ case. The thin vertical line indicates the calculated Fermi level of the system.

FIG. 3. Conductance G for Al DBAT devices. Dashed line: for $d = 2.6\text{a.u.}$; dotted line: $d = 3.9\text{a.u.}$; long dashed line: $d = 5.2\text{a.u.}$; solid line: $d = 6.5\text{a.u.}$. Inset: schematic plot of the atomic DBAT device: an atom is sandwiched in between two metallic wires. The thin vertical line indicates the calculated Fermi level of the system.

Figure 1

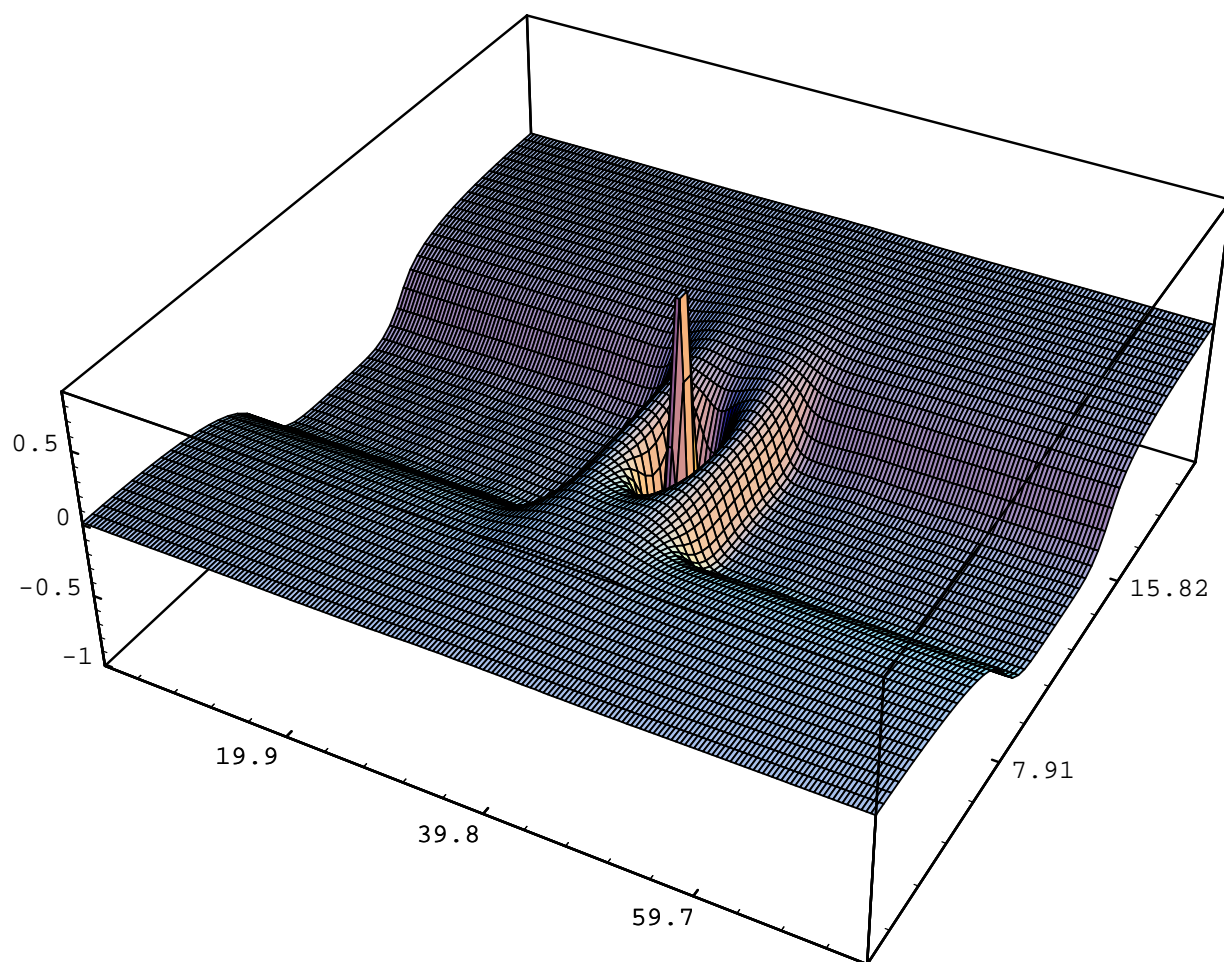


FIGURE 2

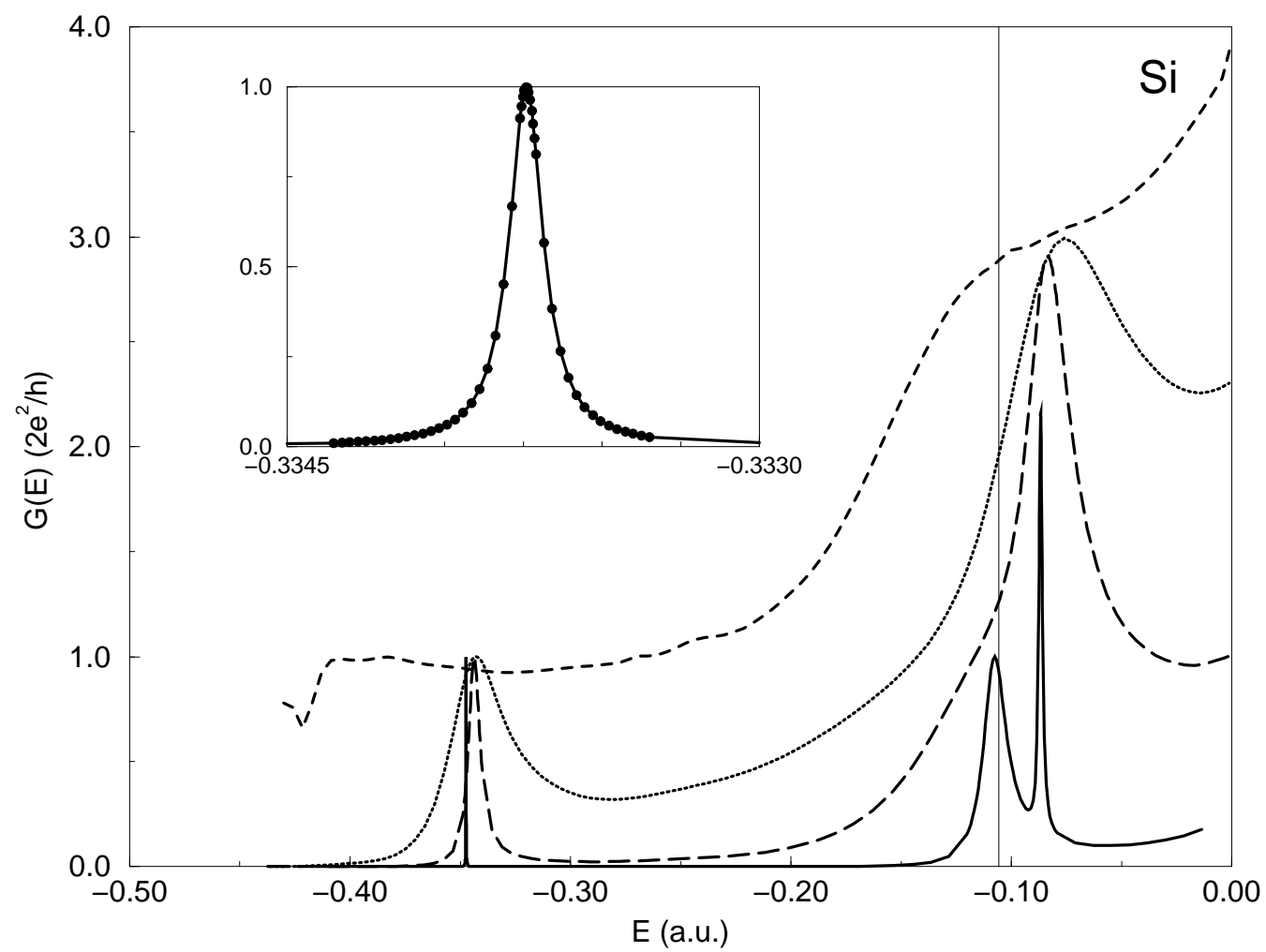


FIGURE 3

